Journal of Quantitative Spectroscopy & Radiative Transfer 310 (2023) 108730

Contents lists available at ScienceDirect

Journal of Quantitative Spectroscopy and Radiative Transfer

journal homepage: www.elsevier.com/locate/jqsrt

Mid-infrared cross-sections and pseudoline parameters for *trans*-2-butene (2-C_4H_8)

Brendan L. Steffens [a,c,d,*], Keeyoon Sung [b], Michael J. Malaska [b], Rosaly M.C. Lopes [b], Geoffrey C. Toon [b], Conor A. Nixon [a]

[a] NASA Goddard Space Flight Center, Planetary Systems Laboratory, Code 693, Greenbelt, 20771, MD, USA
[b] Jet Propulsion Laboratory, California Institute of Technology, 4800 Oak Grove Drive, Pasadena, 91109, CA, USA
[c] Florida Institute of Technology, 150 W University Blvd, Melbourne, 32901, FL, USA
[d] Max Planck Institute for Chemistry, Hahn-Meitner-Weg 1, Mainz, 55128, Germany

ARTICLE INFO

Keywords:
Laboratory spectroscopy
Pseudoline
Cross-sections
Hydrocarbons
Planetary atmospheres
Titan

ABSTRACT

We measured cross-sections for *trans*-2-butene (*trans*-2-C_4H_8: CH_3-CH=CH–CH_3) in the mid-infrared (800–1533 cm^{-1}) in support of remote sensing of Titan's atmosphere. *Trans*-2-butene is one of many C_4 hydrocarbons that is predicted to be present in Titan's atmosphere in detectable abundance, but it has also eluded detection thus far. We collected 20 pure and N_2-mixture spectra at temperatures between 180–297 K using a high-resolution Fourier transform spectrometer (Bruker IFS 125 HR) at the Jet Propulsion Laboratory. Spectral resolutions were selected between 0.0039 and 0.062 cm^{-1}, depending on sample pressures. We observed several fundamental modes of vibration and compared their updated band centers against those previously reported in the literature. Our observations span the 800–1533 cm^{-1} range, which contains multiple vibrational bands and hot band features, and we report temperature-dependent cross-sections in this spectral range. To ensure that our cross-section results are reliable measures of band intensities, we also collected an additional set of 8 room temperature N_2-mixture spectra, investigating the linearity between integrated absorbance and optical burden. We fit all of the observed spectra simultaneously to derive a single set of pseudoline parameters, which include intensities and lower-state energies at separate frequency bins, which are considered as pseudoline positions. The pseudolines are observed to be able to reproduce the observed spectra via line-by-line radiative transfer calculations to within a few percent across the spectral region. The pseudoline list is compiled in HITRAN database format, making it readily integrable in existing radiative transfer codes. The absorption cross-sections represented by the pseudolines provide important laboratory input to the search for elusive molecules in future observations with JWST/MIRI or ground-based observatories such as NASA's Infrared Telescope Facility, as well as in the Cassini/CIRS data archive.

1. Introduction

Titan, the largest moon of Saturn, maintains a thick nitrogen-based atmosphere with a rich organic chemistry. With an enormous variety of organic species contributing to that atmosphere, Titan's chemistry has definite astrobiological implications [1–4]. This complex atmosphere is also known to potentially serve as an analog to the prebiotic atmosphere of the early Earth [5,6]. In this way, Titan serves as a present day laboratory in which to study conditions that possibly contributed to the only known case of biogenesis.

Titan's atmospheric chemistry is initiated via photolysis and photosensitized dissociation of methane (CH_4) and molecular nitrogen (N_2) in the upper atmosphere by solar UV radiation and charged particles accelerated by Saturn's magnetic field. Various chain reactions take place, starting from the simple hydrocarbon and nitrile species produced in the upper atmosphere by these processes. These intermediate reactions inevitably result in larger and more complex species, ultimately contributing to Titan's well-known stratospheric haze layers [7–10].

Understanding the composition of Titan's atmosphere is achieved via a combination of in-situ measurements like those of the Huygens lander [11], remote sensing from flybys, e.g. Voyager mission [7], and from orbiters, e.g. Cassini mission [8,12,13], as well as from space observatories, such as the Infrared Space Observatory [14], and also ground-based observations, e.g. NASA's Infrared Telescope Facility (IRTF) [15] and the Atacama Large Millimeter Array (ALMA) [16]. A last and crucial part of the process, to be described in this paper,

* Corresponding author at: Max Planck Institute for Chemistry, Hahn-Meitner-Weg 1, Mainz, 55128, Germany.
E-mail address: Brendan.Steffens@MPIC.de (B.L. Steffens).

https://doi.org/10.1016/j.jqsrt.2023.108730
Received 24 February 2023; Received in revised form 11 June 2023; Accepted 17 July 2023
Available online 21 July 2023

is laboratory spectroscopy [17–19]. Photochemical models are able to generate predictions regarding the abundances of undetected gases in an atmosphere, and these species can then be studied more closely in the laboratory in order to facilitate their detection in later work.

The molecule of study here, *trans*-2-butene (*trans*-2-C_4H_8: CH_3–CH=CH–CH_3), is one of many C_4 hydrocarbons predicted to be present in detectable abundances within Titan's stratosphere [20–22]. In spite of this, it has not been definitively identified. In an interesting possible connection between Titan's atmosphere and surface features, butene molecules are estimated to contribute up to 1% by volume of Titan's hydrocarbon lakes and seas [23]. These long-standing liquid surface-features render Titan one of the most unique places in the Solar system and a compelling target for further exploration [24]. In another interesting role that butene may play at Titan, it has also been demonstrated that C_4H_8 molecules are a likely product of irradiation of ethane (C_2H_6) ices in cold, Titan-like conditions [25].

Concerning atmospheric butene, the recent photochemical model from Loison [26] and Dobrijevic et al. [22] predicts an abundance of 1 ppb in Titan's stratosphere, at an altitude of 200 km. The much earlier photochemical work of Yung et al. [20] predicts a slightly larger abundance of 6.3 ppb for stratospheric butene. A more recent study [27] predicted a butene abundance of about 10 ppb. Butene molecules are also incorporated in the models of Krasnopolsky [28] and Vuitton et al. [21], though specific stratospheric abundances predicted by these models were not reported.

In order to investigate the abundances of *trans*-2-C_4H_8 and other molecules in Titan's stratosphere from space and ground-based observations, high quality laboratory spectra are required. Preferably, this is done at a range of temperatures and pressures that is representative of Titan's stratosphere. We obtained such a set of 28 *trans*-2-butene spectra between temperatures of 180 K and 297 K, in support of remote sensing of Titan's stratosphere, where temperatures range from about 150 K to 230 K, and pressures range from 10 mbar to 0.1 mbar. After initial data collection, major vibrational bands were identified and compared to previous assignments reported in the literature. We also measured temperature-dependent cross-sections for these vibrational bands, which can be used toward the possible identification of this molecule in NASA IRTF observations, or upcoming mid-infrared spectral observations of Titan from JWST/MIRI [29], for example.

As an additional step toward making these cross-section results more useful through line-by-line calculations, we have also generated a list of spectroscopic pseudoline parameters, compiled in the same format as the HITRAN spectral line database [30]. These pseudolines will serve as a useful alternative to true spectroscopic parameters in radiative transfer calculations, until those become available.

In Section 2, we outline and discuss the experimental details and conditions for our work. In Section 3, we discuss the measurement of the *trans*-2-butene absorption cross-sections and display several examples of these results, as well as an example of the transmission spectra collected. Then, in Section 4, we discuss the derivation of the pseudoline list. In Section 5, we offer a general discussion of the results of our investigation, the significance of this work and its implications, as well as future work which is suggested by our results. Finally, in Section 6, we present our conclusions.

2. Experimental details

We obtained 20 high-resolution spectra (Table 1) of pure *trans*-2-butene and its admixtures with N_2 at temperatures between 297 K and 180 K, in increments of about 30 K, using a Fourier-transform infrared spectrometer (FT-IR), Bruker IFS-125HR, at the Jet Propulsion Laboratory (JPL). The *trans*-2-butene sample (CAS No. 624-64-6) was purchased from Sigma Aldrich, Inc., and is described as having purity of ≥99%. During the acquisition of data, we found distinctive features from the ν_2 band of CO_2 near 667 cm^{-1}. Fortunately, the ν_2 band of CO_2 is highly localized and far from the vibrational features of *trans*-2-butene which we investigated. Furthermore, by simulating CO_2 spectra, we were able to estimate the amounts of CO_2 contributing to each of the *trans*-2-butene spectra we collected, which were taken into account in the cross-section measurements, as to be described in Section 3. These CO_2 partial pressure estimates are also shown in Table 1.

Out of the 20 *trans*-2-butene spectra we collected, 13 were broadened with research-grade (99.999995%) N_2 gas. We note here that this choice is appropriate, given Titan's atmospheric composition, which is dominated by molecular nitrogen (greater than 98% by volume) [11]. The spectral resolutions we used were selected in consideration of several factors. In particular, Doppler widths and estimates of Lorentz widths at the given pressures and temperatures presented in Table 1, and the signal-to-noise ratio to be achieved. As a rule of thumb, we obtained the N_2-admixture spectra at lower spectral resolutions than the pure *trans*-2-C_4H_8 spectra in order to enhance S/N, as long as these settings were able to capture the details of the key vibrational features. For pure sample spectra at low pressures, for which the Doppler broadening is very small, we adopted a very high spectral resolution (e.g. 0.0039 cm^{-1}), but not as high as the Doppler width equivalent, to achieve high S/N and secure high precision measurements. This approach is acceptable because most of the *trans*-2-butene rovibrational transitions are observed to be substantially smeared out, rendering all lines substantially blended. Thus, their effective line widths are much greater than the theoretical Doppler width expected for an isolated line. Overall, the peak-to-peak S/N values achieved were 80:1 or better for pure sample spectra in high resolution and 300:1 or better for N_2-mixture spectra at low resolution (see Table 1 for spectral resolutions).

We employed the same cold copper gas cell that we have made use of in our previous work on Titan's other hydrocarbons, such as *n*-butane (*n*-C_4H_{10}) [19], propane (C_3H_8) [17], and propene (C_3H_6) [18]. We include only a brief description of the gas cell here. The cell is bracketed by a pair of wedged ZnSe windows and housed in a separate vacuum shroud with KBr windows, which protects the cell windows from collecting cryodeposits at cold temperatures. The temperature of the gas cell was regulated via a closed-cycle helium-cooled refrigerator and a heater attached to the body of the cell. A pair of silicon-diode temperature sensors were also attached to the cell body: the first of these is close to a heat reservoir connected to the cold finger of the gas cell to provide a temperature control feedback loop, and the other is attached to the cell body farthest away from the heater, to be used as an indicator of gas sample temperature. Excellent temperature regulation was observed during our study (typically, stability was better than 0.1 K over several days). A more detailed characterization and performance of this gas cell can be found elsewhere [e.g. 17,19].

In order to compensate for the 99% sample purity of the *trans*-2-butene sample that we used in this study, and to investigate the possibility of additional contamination beyond the 1% level in our sample, we simulated the ν_2 band of CO_2 under the experimental conditions of each of our spectra. We then used these simulated spectra to determine the partial pressure of CO_2 contributing to each spectrum. These partial pressures (see Table 1) were then used in correction factors when computing the cross-sections for that particular spectrum and when fitting the spectra during the derivation of the pseudoline list. We also checked the sample for possible impurity from O_2 and N_2, using the classic freeze-and-thaw method. Unlike the case of CO_2, we have found the combined maximum abundance of O_2 and N_2 is 0.1%, which has turned out to be insignificant in comparison to our other measurement uncertainties.

In Table 2, we summarize the instrumental parameters for our interferometer, a Bruker 125HR, which was configured with a Globar infrared source, a KBr beam splitter, and a liquid N_2-cooled MCT (Mercury Cadmium Telluride) detector. Maximum optical path differences of 128.57, 50.00, 41.67, and 8.04 cm were used, providing unapodized spectral resolutions of 0.0039, 0.010, 0.012, 0.062 cm^{-1}. We used an

Table 1
Experimental conditions of pure and N_2-broadened *trans*-2-butene spectra. Each spectrum used a path length of $L = 20.38$ cm.

Pure/N_2-Mix	Spectrum	T (K)	P_s (Torr)	P[CO_2] (Torr)	P_t (Torr)	Resolution (cm^{-1})
Pure	B0189.1a	297.0(1)	12.68(1)	0.27	12.95(1)	0.0100
	B0189.1b	297.6(1)	5.33(1)	0.10	5.43(1)	0.0039
	B0189.1c	297.0(2)	5.33(1)	0.11	5.44(1)	0.0100
	B0189.2a	278.2(1)	4.00(1)	0.04	4.00(1)	0.0039
	B0189.3a	240.1(1)	1.99(1)	0.02	2.01(1)	0.0039
	B0189.4a	210.1(1)	1.39(1)	0.01	1.40(1)	0.0039
	B0189.7a	180.0(1)	0.60(1)	0.00	0.60(1)	0.0039
Mixture	B0189.1d	297.3(1)	5.33(1)	0.10	760.9(1)	0.0620
	B0189.1e	297.6(1)	5.33(1)	0.10	765.3(1)	0.0560
	B0189.1f	297.5(3)	6.96(1)	0.11	120.0(1)	0.0120
	B0189.1g	297.9(1)	6.96(1)	0.11	234.5(1)	0.0120
	B0189.2b	278.2(1)	4.92(1)	0.08	118.5(1)	0.0120
	B0189.2c	278.2(1)	3.95(1)	0.05	239.5(1)	0.0120
	B0189.2d	278.2(1)	4.82(1)	0.18	763.4(1)	0.0620
	B0189.3b	240.1(1)	2.98(1)	0.05	120.2(1)	0.0120
	B0189.3c	240.1(1)	2.95(1)	0.08	760.6(1)	0.0620
	B0189.4b	210.1(1)	1.79(1)	0.02	109.7(1)	0.0120
	B0189.4c	210.1(1)	1.78(1)	0.03	759.8(1)	0.0620
	B0189.7b	180.0(1)	0.59(1)	0.00	100.0(1)	0.0120
	B0189.7c	180.0(1)	0.59(1)	0.01	299.6(1)	0.0620
	B0189.8a	297.7(1)	0.5(1)	0.01	760.0(1)	0.0620
	B0189.8b	298.0(1)	0.99(1)	0.00	760.2(1)	0.0620
	B0189.8c	298.3(1)	1.99(1)	0.02	759.3(1)	0.0620
	B0189.8d	297.2(1)	3.54(1)	0.04	760.2(1)	0.0620
	B0189.8e	297.3(1)	7.84(1)	0.06	760.2(1)	0.0620
	B0189.8f	297.7(1)	11.95(1)	0.08	760.0(1)	0.0620
	B0189.8g	296.9(1)	18.01(1)	0.13	761.1(1)	0.0620

Table 2
Instrumental configuration of the Bruker 125HR and cold gas cell.

Spectral region	650–1550 cm^{-1}
IR source	Globar
Beam splitter	KBr
Resolutions	0.0039, 0.010, 0.012, 0.062 cm^{-1}
Aperture diameter	2.0 mm
Cell length	20.38 cm
Windows (wedged)	ZnSe on cell, KBr on vacuum shroud
Detector	HgCdTe (cooled by liquid N_2)
Sample and purity	*trans*-2-C_4H_8 (99%), N_2 (99.9999%)
FTS chamber	Evacuated down to ~10 mTorr (mostly residual H_2O)

optical filter which encompasses the 650–1550 cm^{-1} part of the mid infrared in order to obtain the desired bandpass. For convenience of analysis and discussion, we separate this bandpass into two Regions, with Region 1 being 800–1120 cm^{-1}, and Region 2 being 1120–1533 cm^{-1}. The aperture diameter was set to 2.0 mm for all spectra that we collected. The entire path of the optical beam through the Bruker FT-IR chambers was evacuated to pressure of approximately 10 mTorr during the data acquisition.

We monitored sample pressures continually using three sets of MKS Baratron transducers with 0–10, 0–100, and 0–1000 Torr pressure ranges. Pressures were observed to be very stable during the data collection process, indicative of a well-sealed system. We selected a variety of total pressures and sample volume mixing ratios in order to obtain sufficient optical depth for the respective experimental conditions, which were listed in Table 1. Pure sample spectra were collected at a given temperature, and then followed by admixture spectra after insertion of N_2, executed by a standard procedure designed to minimize uncertainty in the sample partial pressure: the sample inlet tube was first evacuated up to the shut-off valve of the gas cell after each insertion of pure sample. For preparation of admixtures, before adding $N_2$to the cell, we pressurized the sample line with N_2 up to the gas cell shut-off valve, effectively preventing any possible back-flow of the *trans*-2-butene already present in the gas cell. Partial pressure of the *trans*-2-butene sample was obtained from the initial pressure measurement of the pure *trans*-2-butene sample for the ensuing admixture spectra.

During the addition of both sample and N_2, the gas was fed first through a copper coil submersed in a dry ice/methanol (CH_3OH) slurry which was continuously kept at a temperature of about 245 K. This forced any water vapor sample impurity to condense onto the copper coil, rather than entering the gas cell. The absorption contribution of water impurity to the cross-sections that we report was largely made negligible due to this process. Most residual water features from the FTS chambers were later canceled out when each sample spectrum was normalized to its corresponding background spectrum. Note also that the dry ice/methanol slurry temperature was kept sufficiently *warm* enough such that the *trans*-2-butene sample would not also condense out (*trans*-2-butene's vapor pressure is approximately 110 Torr at 245 K). For this, we utilized *trans*-2-butene vapor pressure data from Shimanouchi et al. [31].

The range of temperatures explored in this study (180–297 K) was selected to provide a broad range appropriate to remote sensing within the atmospheres of both Titan and Earth. Additionally, this temperature range was used to ensure proper sample pressures producing sufficient optical density, without any significant part of the measured absorption features becoming saturated. Finally, the data provided by Shimanouchi et al. [31] also informed our decision to keep experimental temperatures *above* 180 K; keeping temperatures above 180 K ensured that no condensation would occur inside the gas cell, eliminating a major source of uncertainty.

3. Cross-section measurements

With $N = 12$ atoms, the *trans*-2-C_4H_8 molecule has $3N - 6 = 30$ cold fundamental vibrational modes, listed in Table 3. Many of the locations and relative strengths of the *trans*-2-C_4H_8 bands (along with those of the isomer *cis*-2-C_4H_8) were measured several decades ago by McKean et al. [32]. However, seven of *trans*-2-butene's 30 vibrational modes were not discussed in that study, and since then, it seems that little work has been performed to actually remeasure any of the band centers. The band centers of both *cis*- and *trans*-2-C_4H_8 were later *calculated* by Chhiba and Vergoten [33] using the SPASIBA molecular mechanics potential [34]. The C_4H_8 isomer 1-butene (CH_2=CH–CH_2–CH_3), on the other hand, was studied more recently in the far infrared by Bell et al.

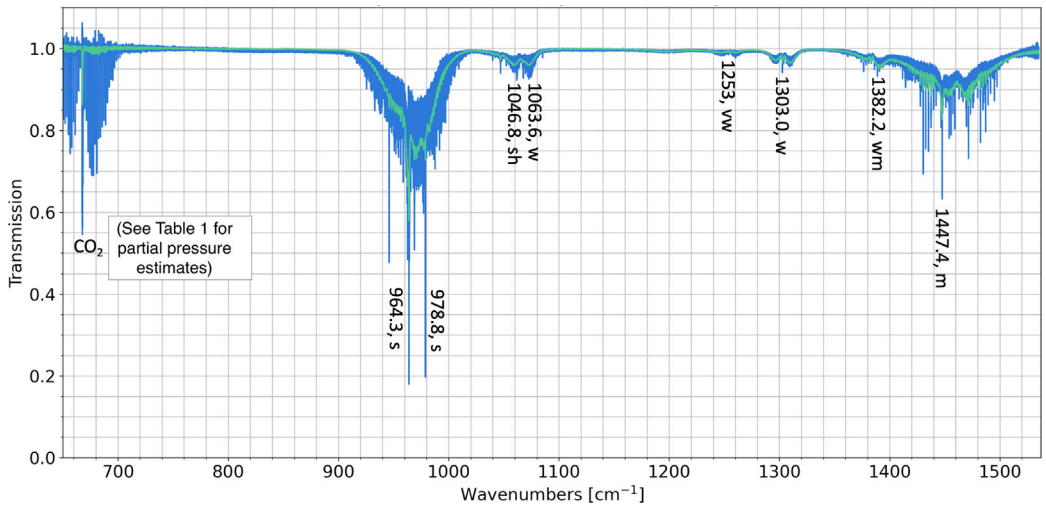

Fig. 1. Sample of pure and N_2-mixture spectra of *trans*-2-C_4H_8 obtained at 210 K. The pure spectrum (blue curve) was obtained with sample pressure P_s = 1.39 Torr at resolution 0.0039 cm^{-1}, where as the N_2-broadened spectrum (green curve) was obtained with sample pressure P_s = 1.78 Torr, total pressure P_{tot} = 759.8 Torr, at resolution 0.062 cm^{-1}. Several representative band centers for *trans*-2-C_4H_8 are identified, using the notation of [32] (i.e. s = strong, vw = very weak, etc.). Note that the features around 667 cm^{-1} are contamination from CO_2. The partial pressure contributions from CO_2 to the spectra are shown (in the same color scheme), estimated by simulating CO_2's ν_2 band.

Table 3
Measured band centers of trans-2-butene fundamentals (in cm^{-1}), adopted from Barnes and Howells (1973) [36].

Bands	Symmetry A_g	Bands	Symmetry B_g
1	3011	16	2948
2	2954	17	1457
3	2930	18	1043
4	1680	19	750
5	1385	20	210
6	1309	Bands	Symmetry B_u
7	1138		
8	864	21	3036
9	501	22	2976
Bands	Symmetry A_u	23	2892
		24	1457
10	2950	25	1455
11	1444	26	1379
12	1024	27	1306
13	975	28	1069
14	240	29	966
15	133[a]	30	290

[a]Calculated value adopted from [33].

[35], through which band centers and their associated symmetries and vibrational modes have been established for that particular molecule.

15 of the 30 fundamental vibrational modes as listed in McKean et al. [32] lie within the spectral range studied here; we were able to confirm eight of those bands. An example of the identification of these bands can be seen in Fig. 1. It can be seen that *trans*-2-butene's strongest vibrational feature in the studied region is the set of bands near 970 cm^{-1}. These are the most promising targets in the pursuit of identification of this molecule in remote observations of Titan, because this region is relatively free from other known hydrocarbons, excepting ethylene (C_2H_4) [37].

Cross-sections, denoted by σ_ν and measured in cm^2 mol^{-1}, are derived from an observed transmission spectrum τ_{obs}, which is described via the Beer–Lambert law,

$$\tau_{obs}(\nu) = \exp(-\sigma_\nu n \xi L), \quad (1)$$

where n is the total number density (in molecules cm^{-3}), ξ is the volume mixing ratio of *trans*-2-butene, and L is the absorption path length (20.38 cm for all of the spectra discussed in this paper). Samples of the derived cross-sections are shown in Figs. 2 and 3. The two regions displayed carry significant contributions from numerous vibrational bands (either cold, hot and combination bands), most of which remain unidentified at this time. The rovibrational transitions of these bands are smeared out (along with the cold fundamental bands) to produce the continuum-like absorption bands.

As a test of the reliability of the collected cross-section data, we also obtained an additional set of room temperature, N_2-mixture spectra, each with total pressure of approximately 760 Torr, but with varying amounts of *trans*-2-C_4H_8 sample (Spectra 8a–8g, see Table 1). As suggested in the PNNL database [38], as well as by Varanasi (1976) [39] and Varanasi & Chudamani (1987) [40], we used this data set to test the linearity between the integrated absorbance and the optical burden (defined as the product of gas sample pressure and the gas cell's path length). For sufficiently small optical burdens, the integrated absorbance for a given spectral region is proportional to the optical burden, with the slope of the relationship being the band intensity itself. All of our cross-section measurements were derived from spectra that satisfy this linearity condition, and are thus suitable for reporting band intensities. The results of this test are shown in Fig. 4. The quality of linear fit, detailed in the legend, is measured by R^2 = 0.99987, with standard deviation of the residuals between the absorbances and the fit being σ = 0.07.

As a final step, we also used Spectra 8a–8g to calculate the integrated cross-section of Region 1 and Region 2 separately, via linear regression. As mentioned previously, the slope of the relationship in Fig. 4 is the band intensity for the band being measured, or the integrated cross-section, in the case of coverage of a larger wavenumber interval which contains several different absorption bands. Thus, we investigated this relationship for spectra 8a–8g, first for Region 1 and then for Region 2, obtaining integrated cross-section values of 8.16(15)×10^{-18} cm^2 mol^{-1} and 6.06(16)×10^{-18} cm^2 mol^{-1}, respectively.

4. Pseudoline generation

In addition to our cross-section results, we have also taken the empirical pseudoline generation approach and developed a HITRAN-formatted pseudoline list. The pseudoline approach was originally introduced by Toon et al. [41,42] and has since been employed in the analysis of laboratory spectra of hydrocarbons [18,19,43], as well as in atmospheric remote sensing [44–46]. A pseudoline parameterizes absorption features measured in the laboratory. We describe the method

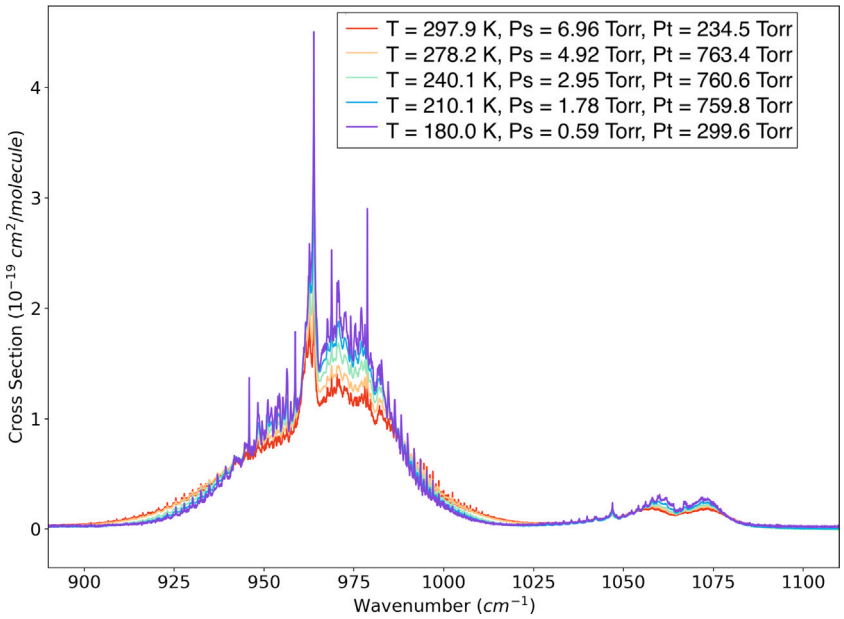

Fig. 2. Sample of cross-sections for *trans*-2-C_4H_8 (890–1115 cm^{-1}) derived at cold temperatures, with cooler colors denoting colder temperatures.

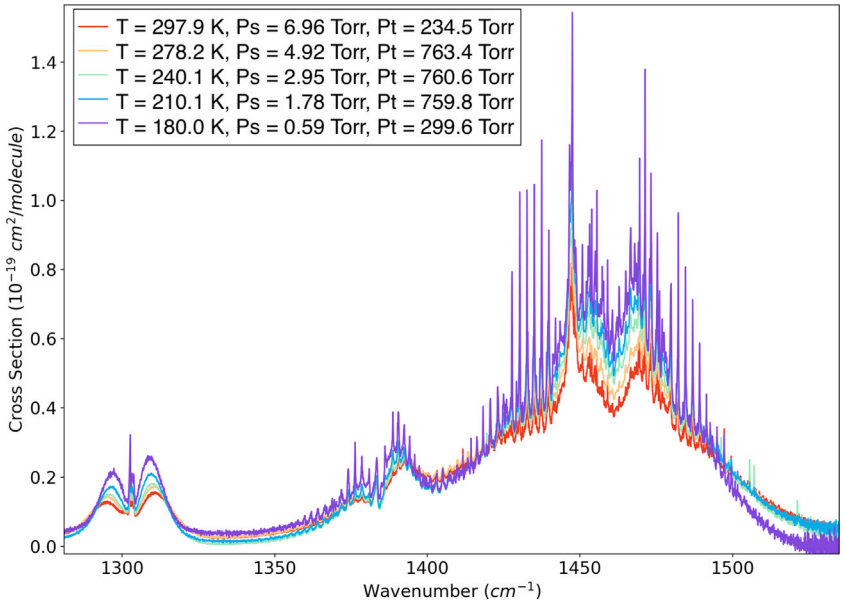

Fig. 3. Sample of cross-sections for *trans*-2-C_4H_8 (1285–1533 cm^{-1}) derived at cold temperatures, with cooler colors denoting colder temperatures.

here briefly: from laboratory spectra, the mean observed coefficients across a narrow wavenumber interval are modeled by a set of 'effective' line parameters, including lower state energy E" and line intensity S. The Voigt lineshape profile is adopted for the pseudolines. The pseudoline parameters become more robust when they are derived from experimental data which covers a wide range of temperature and pressure.

Several advantages are provided by the pseudoline method over cross-sections measured at a set of discrete temperatures and pressures. For instance, the pseudoline list, as it has been derived by fitting multiple spectra using the Voigt line shape profile as well as the instrument's line shape function, is independent of both spectral resolution and instrument choice. Additionally, artifacts arising from impurities, such as the transitions observed in this work from CO_2 and water vapor, or channel fringes, can be removed during the fitting of the spectra, which prevents their contributions from contaminating the pseudoline list. A final advantage is that the pseudoline list is compiled in a HITRAN-compatible format, and is readily usable in existing radiative transfer line-by-line calculations. Further information on the pseudoline method can be found on the JPL MK-IV website: http://mark4sun.jpl.nasa.gov/data/spec/Pseudo/Readme.

Using a frequency grid spacing of 0.01 cm^{-1}, we fit all 27 of the *trans*-2-C_4H_8 spectra in order to generate the pseudoline parameters. This spacing for the frequency grid is a compromise between retrieval precision and computation expense. We note that 0.01 cm^{-1} spacing is fine enough to capture detailed spectroscopic features observed by Cassini/CIRS, which featured a highest apodized spectral resolution of 0.5 cm^{-1} [13]. At each point on the frequency grid, an effective intensity S [in cm^{-1}/(mol cm^{-2})] and lower state energy E" [in cm^{-1}] have been derived for that respective pseudoline. As in our previous work with similar hydrocarbons, we assumed values of 0.12 and 0.18 cm^{-1}/atm at 296 K for the N_2- and self-broadened line widths of *trans*-2-C_4H_8, borrowed from early measurements of collisional broadening

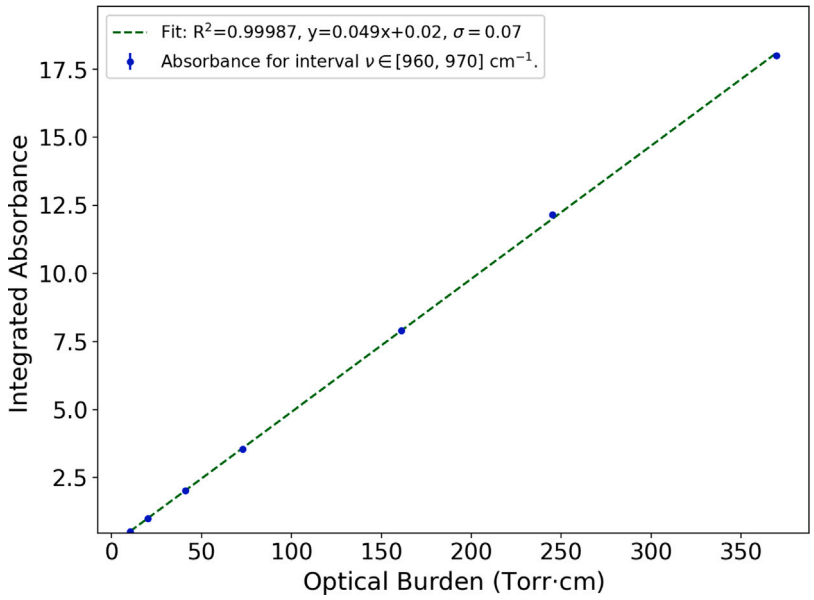

Fig. 4. Test of linearity between integrated absorbance and optical burden (defined as gas sample pressure times cell path length). This test was conducted using a set of separate room temperature spectra (Spectra 8a–8g, see Table 1), each with total pressure of approximately 760 Torr. The spectral range covered here is just 960–970 cm^{-1}, which features the strongest rovibrational features (band 29, Table 3) in the full spectral region studied.

of propane (C_3H_8) by N_2 [47]. We assumed a value of $n = 0.75$ for the temperature dependence exponents for these values, as in $\gamma(T) = \gamma°(296\ K) \times (296/T)^n$.

A monochromatic spectrum is computed using the Voigt line shape profile, which is then convolved with the instrument line shape function (sinc function with a field-of-view correction). The pseudoline intensities are compiled at a reference temperature of $T_0 = 296$ K. Then, the intensity at another temperature T is calculated via Eq. (2),

$$\frac{S(T)}{S_0} = \frac{[Q_t(T_0)]}{[Q_t(T)]} \frac{[\exp(-c_2 E\varepsilon/T)]}{[\exp(-c_2 E\varepsilon/T_0)]} \frac{[1-\exp(-c_2\nu/T)]}{[1-\exp(-c_2\nu/T_0)]}, \quad (2)$$

in which Q_t is the total partition function for *trans*-2-C_4H_8 , $c_2 = 1.4388$ cm/K is the second Boltzmann constant, and ν is the position of the pseudoline. The total partition function is computed as the product of the vibrational partitional function and the rotational partition function, i.e. $Q_t = Q_{vib} \times Q_{rot}$. For the vibrational partition function, we made use of the Harmonic Oscillator approximation, expressed in Eq. (3),

$$Q_v(T) = \prod_n \left[\frac{1}{1-\exp(-c_2 E_{v,n}/T)}\right]^{\delta} \quad (3)$$

where the index n runs over the 30 vibrational modes of *trans*-2-C_4H_8. The degeneracy, δ, is unity for all n for *trans*-2-C_4H_8. $E_{v,n}$ is the band center of the nth vibrational mode (Table 3). The ratio of rotational partition functions (for two different temperatures) is approximated by Eq. (4),

$$\frac{Q_{rot}(T)}{Q_{rot}(296K)} = \left(\frac{T}{296K}\right)^{\beta} \quad (4)$$

where β is the temperature dependence exponent. For polyatomic species which have one or more torsional modes, such as *trans*-2-C_4H_8, $\beta = 2$; this accounts for the contribution from those torsional modes and their interaction with the other vibrational modes, enhancing the total partition function.

A brief excerpt from the pseudoline list (for Region 1) is displayed in Table 4 in order to show how the parameters for each line are arranged. These parameters are: molecular index, isotopologue index, line position, line intensity, and lower state energy, followed by the various pressure-broadened width values described previously and adopted for this work.

Table 4
Sample of HITRAN-formatted pseudoline list derived in this work.

```
------------------------------------------------------------------------
MMI  freq(cm-1) S (296 K)       Widths      E"    n  N2-shift
------------------------------------------------------------------------
820  800.000000 3.534E-23 0.000E+00.1200.1800  790.18890.75-.003000
820  800.010000 1.446E-24 0.000E+00.1200.1800  851.15590.75-.003000
820  800.020000 1.490E-24 0.000E+00.1200.1800  819.79790.75-.003000
820  800.030000 1.869E-24 0.000E+00.1200.1800  956.47170.75-.003000
820  800.040000 7.930E-25 0.000E+00.1200.1800  802.66410.75-.003000
820  800.050000 1.057E-25 0.000E+00.1200.1800  497.58820.75-.003000
820  800.060000 1.044E-25 0.000E+00.1200.1800  542.44940.75-.003000
820  800.070000 1.328E-25 0.000E+00.1200.1800  559.38780.75-.003000
820  800.080000 1.315E-25 0.000E+00.1200.1800  506.47650.75-.003000
820  800.090000 1.714E-25 0.000E+00.1200.1800  705.79250.75-.003000
------------------------------------------------------------------------
```

Note: As an example, the first row should be read as line position = 800.000000 cm^{-1}, line intensity=3.534E−23 cm^{-1}/(mol cm^{-2}), N_2-width=0.1200 cm^{-1}/atm, self-width=0.1800 (cm^{-1}/atm), E"=790.18890 cm^{-1}, n = 0.75, N_2-shift= -.003000 cm^{-1}/atm. Note that the widths and shift are assumed, and that the fourth column is a placeholder for the Einstein coefficient. Additional details on the data format can be found on the HITRAN database [30].

It must be noted that though all 27 spectra were used in the pseudoline list derivation for Region 1, the three spectra at temperature 180 K (spectra 7a, 7b, 7c) were omitted from the derivation of pseudolines in Region 2. This is due to particular difficulty in baseline determination for these spectra, which suffered from large amounts of noise at the high wavenumber end of the bandpass. This is discussed more thoroughly in the following section.

Figs. 5 and 6 show fits to the laboratory spectra using the derived pseudolines and the resulting spectral fitting residuals, for Regions 1 and 2, respectively. We note that the residuals are vertically symmetric, implying they are due to spectral noise and the pseudoline frequency grid (i.e. 0.01 cm^{-1}) being insufficient to capture fast amplitude variations in the spectra at very high spectral resolution (i.e. 0.0036 cm^{-1}). As seen in the left panel of Fig. 5, the fitting residuals are better than 5% for all the N_2-mixture spectra, which is consistent with the measurement uncertainty (~6.4%) that we estimate from the Volume mixing ratio Scale Factors for Region 1, which are discussed in Section 5 and shown in Fig. 7. The same is true of Region 2 (Fig. 6), where residuals are well below 5%, consistent with the corresponding measurement uncertainty of 5.4% estimated later.

In addition to the optomechanical stability of our spectrometer and the reliability of our sensors, our measurement uncertainty reported

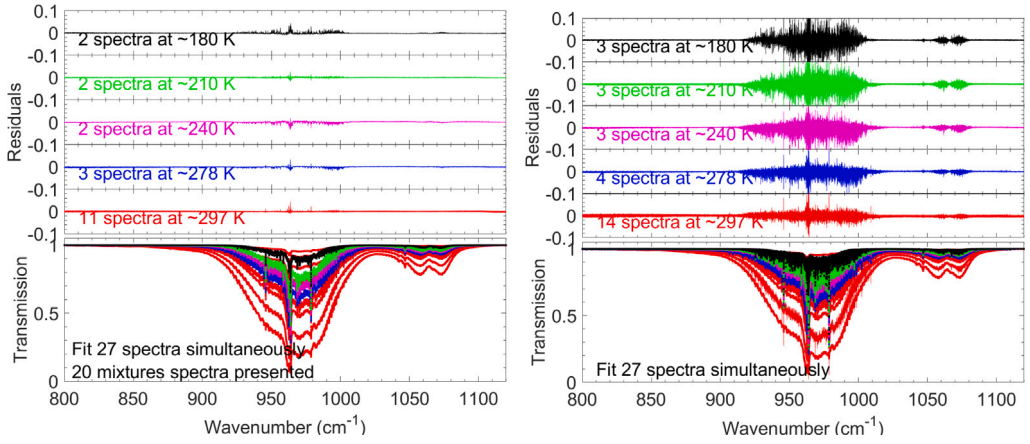

(a) Mixture spectra only (b) Pure and mixture spectra

Fig. 5. Fitting residuals, sorted by measurement temperatures, for Region 1 (800–1120 cm^{-1}). Panel (a) shows the fitting residuals for N_2-mixture spectra only, where residuals are seen to be ≤5%. Panel (b) shows the both the pure and mixture spectra, where the fitting residuals are significantly noisier, but vertically symmetric, only affecting the uncertainty of the measurements.

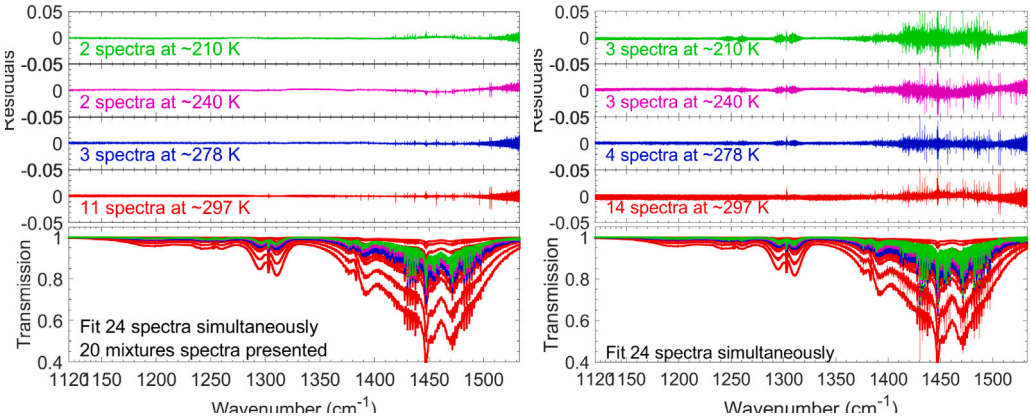

(a) Mixture spectra only (b) Pure and mixture spectra

Fig. 6. Fitting residuals, sorted by measurement temperatures, for Region 2 (1120–1533 cm^{-1}). Once again, Panel (a) shows the fitting residuals for N_2-mixture spectra only, where residuals are very low, at ≤5%. Panel (b) shows the both the pure and mixture spectra, where the fitting residuals are significantly noisier, but again vertically symmetric.

here was also made possible by the use of a dry ice/methanol slurry. As described in Section 2, gas sample and broadening N_2gas were fed through a copper coil submersed in this chilled bath before entering the gas cell, forcing water impurity in the gas sample to condense out. Removal of residual water vapor from our data was consistently observed, and this facilitated the process of measuring cross-sections for *trans*-2-butene in the 1300–1550 cm^{-1} region without having the cross-section measurements being contaminated by the water.

5. Results and discussion

Though we measured temperature-dependent cross-sections in this study, our primary result is the HITRAN-formatted pseudoline list for *trans*-2-C_4H_8. As a test for the general validity of the pseudoline list, we did multispectrum fitting for all 27 spectra (including those used in the Linearity Test), in order to retrieve Volume mixing ratio Scale Factors (VSF) for the *trans*-2-C_4H_8 sample pressures. In Fig. 7, we show these retrieved VSFs for both spectral Regions 1 and 2. Retrieved VSFs equal to unity would be ideal and confirm that the generated pseudolines correctly represent the spectra obtained at their respective experimental conditions. Any offsets from unity for the VSF can be regarded as uncertainties of the pseudolines as a whole. Therefore, the standard deviation of the VSFs from the 27 spectra can be interpreted as measurement uncertainty for the cross sections computed with the pseudoline list for either Region.

In Fig. 7, the VSFs retrieved are presented for individual spectra for each Region with their retrieval errors as error bars. The standard deviations of the VSFs are calculated to be 6.4% for Region 1, and 5.6% for Region 2, with associated mean values of 1.006 and 0.990, respectively. The mean value for Region 2 indicates a bias of 1%, though this is still dominated by the overall uncertainty of the pseudoline list in that region.

Fig. 8 shows the integrated pseudoline intensities for Region 1 and Region 2 (which are also listed in Table 5), computed by summing the individual pseudoline intensities for those spectral regions. For comparison, our integrated cross-section measurements for N_2-mixture spectra at total pressure of approximately 760 Torr are also shown in this same figure. No cross-section result is plotted for temperature 180 K, as we did not obtain a spectrum with total pressure 760 Torr at that temperature. The uncertainty of the room temperature cross-sections was determined via linear regression. We adopt this same uncertainty for the cross-sections at colder temperatures, assuming similar levels of persistent outgassing/degassing and system performance for those measurements. The figure illustrates that the direct measurements of the cross-sections and the value computed by the pseudoline intensities show fairly good agreement within 10% across the experimental temperatures, except for Region 2 at 180 K. We note that the direct

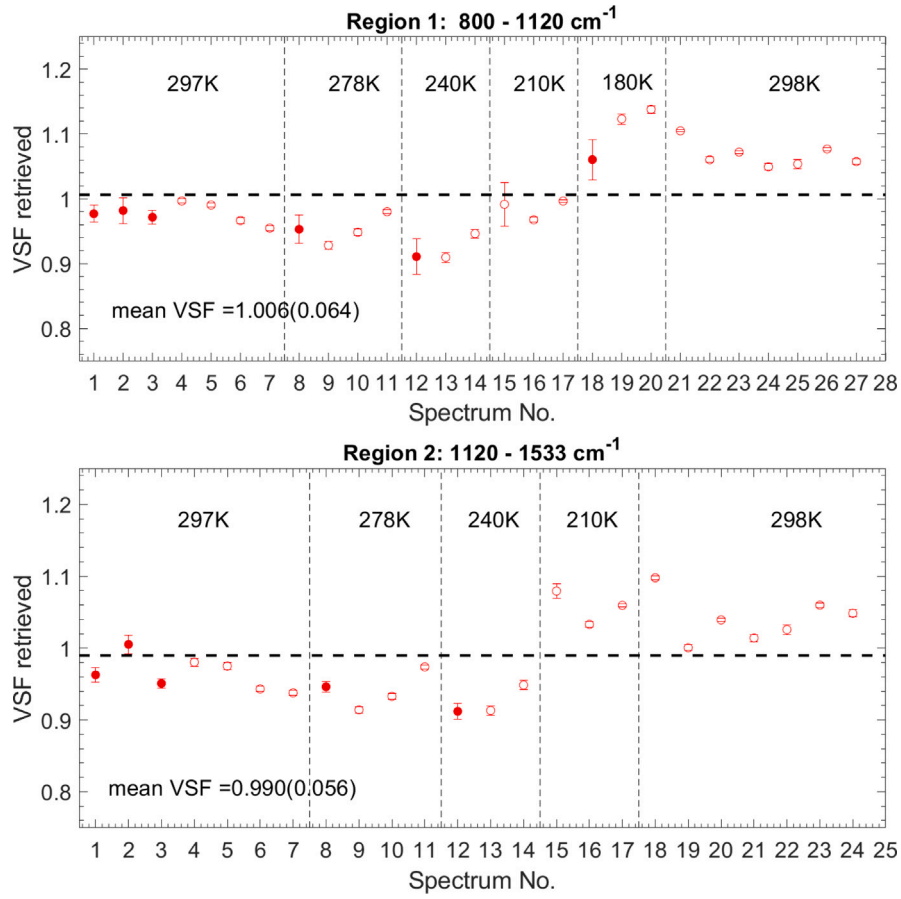

Fig. 7. The retrieved Volume mixing ratio Scale Factors (VSFs) for each of the spectra. Pure *trans*-2-C_4H_8 spectra are marked with solid red circles, whereas N_2-mixture spectra are marked with hollow circles. The mean VSF is shown with a dashed horizontal line. The error bars shown are the retrieval errors for the individual spectra.

cross-section measurements in Region 2 were likely affected by inconsistent baseline corrections beyond the 1500 cm^{-1} point. As hinted at in Figs. 1 and 3, the right side of the bands beyond 1530 cm^{-1} were particularly noisy, being close to the edge of the bandpass filter, which hindered the ability to determine the 100% transmission level for Region 2. This is another reason that the pseudoline lists are superior to the cross-section measurements, because the pseudolines are generated by fitting all the spectra simultaneously for optimum representation of the entire set, intrinsically securing self-consistency.

We reiterate here that due to the baseline-correction problem experienced in Region 2, the three spectra at temperature 180 K were omitted from the generation of the pseudolines, as these spectra were particularly noisy at the high wavenumber end of the bandpass. Thus, Region 1 pseudolines are valid down to temperature 180 K, whereas Region 2 pseudolines are only valid down to temperature 210 K. Fortunately, *trans*-2-C_4H_8 's strongest absorption features are contained in Region 1, and these are the likely targets for the search for *trans*-2-C_4H_8 in Titan's cold stratosphere.

In addition to the intrinsic self-consistency of the pseudolines, the pseudoline list may also be used to model *trans*-2-C_4H_8 at temperatures not explicitly covered in this work. For instance, as stated earlier, the temperatures of Titan's stratosphere where *trans*-2-C_4H_8 is likely to be found ranges from about 150 K to 230 K. The pseudoline list can safely model *trans*-2-C_4H_8 at these colder temperatures, at the cost of up to an approximate 10% increase in uncertainty.

Ding et al. [48] conducted a high-temperature spectroscopic study of both *cis*- and *trans*-2-butene (separately), in addition to several other molecules, for just the 900–1200 cm^{-1} range. Though their purpose was to measure cross-sections at high temperatures, they also obtained one room temperature result as well, at N_2-broadened total pressure of approximately 760 Torr, to which we have compared our results (Fig. 8). When integrated, their room temperature cross-sections for *trans*-2-butene match the average of our room temperature results in the common spectral range (900–1200 cm^{-1}) to within about 7%.

Table 5
Integrated pseudoline intensities [10^{-18} cm^{-1}/(mol cm^{-2})], at the five experimental temperatures used in this study, for both Region 1 (800–1120 cm^{-1}) and Region 2 (1120–1533 cm^{-1}). Uncertainties are calculated as 6.4% and 5.6% for Region 1 and Region 2, respectively, as described in Fig. 7.

Temperature	Region 1	Region 2
296 K	7.82(50)	5.89(33)
278 K	8.29(53)	6.24(35)
240 K	8.72(56)	6.44(36)
210 K	8.38(54)	5.88(33)
180 K	7.34(47)	4.62(26)[a]

[a]This value is an extrapolated estimate, as the T = 180 K spectra were not included in the fitting for Region 2.

We note that no comparison is possible with the room temperature integrated cross-section results by PNNL [38], given that a 60% *trans*-2-C_4H_8 and 40% *cis*-2-C_4H_8 mixture was utilized in that study, and both stereoisomers are spectroscopically distinct.

Similar studies to the one presented here are still required for the four other C_4H_8 isomers (1-butene, 2-methylpropene, cyclobutane, and methylcyclopropane), as well as the other 2-butene stereoisomer (*cis*-2-butene). As each of these species is a possible constituent of Titan's atmosphere and likely plays a unique role in Titan's chemistry and the production/destruction of other important molecules, careful laboratory characterization studies of absorption cross-sections or

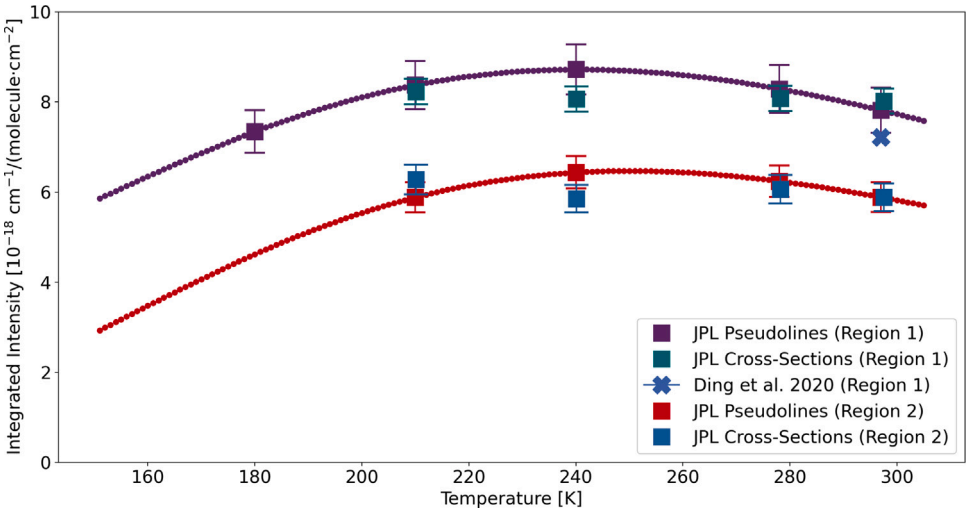

Fig. 8. Integrated pseudoline intensities (cm^{-1}/mol cm^{-2}), with error bars (6.4% and 5.6% for Region 1 and Region 2, respectively, as discussed in Fig. 7. Our cross-section measurements (discussed in Section 3) are also shown in green. In Region 1, the room temperature result for Ding et al. (2020) [48] for pure *trans*-2-C_4H_8 is shown, though no uncertainty is provided for that result. The observed temperature dependent behavior of the pseudolines may be associated with the partition function adopted for *trans*-2-C_4H_8 .

spectral lines are required for each isomer. We note that once such a characterization is achieved for the *cis*-2-butene isomer specifically, that can be combined with our results reported here and compared to the earlier results from PNNL [38], which featured a mixture of both the *trans* (60%) and the *cis* (40%) stereoisomers.

Finally, we reiterate that as these various C_4H_8 isomers are thought to be important potential liquids in the lakes and putative subsurface reservoirs of Titan [23,49], constraining their atmospheric abundances is a reasonable first step toward understanding atmosphere to surface transfer interactions [e.g.50]. Additionally, *trans*-2-C_4H_8 is involved in the production of the chiral molecule *trans*-1,2-dimethylcyclopropane (C_5H_{10}), via a set of reactions that may also take place in the atmosphere of Titan [51,52]. Further study of this reaction scheme and the *trans*-1,2-dimethylcyclopropane molecule specifically would initiate progress toward understanding new, undetected species in Titan's atmosphere.

6. Conclusion

We have measured high resolution infrared absorption cross-sections for the *trans*-2-butene (*trans*-2-C_4H_8) molecule, a likely constituent of Titan's atmosphere according to photochemical models [20,21,26,28]. These cross-sections were measured at a variety of cold temperatures and N_2-broadened pressures suitable for modeling of observations of Titan's atmosphere. Additionally, we derived a HITRAN-formatted pseudoline list for *trans*-2-C_4H_8 that can be readily implemented in radiative transfer modeling codes. Our cross-section results and the pseudoline list are found to be in good agreement. We recommend that the pseudoline list be used in future modeling work, rather than the cross-sections, since the pseudolines are the representative results across the measurement temperature range, they are internally self-consistent, and they can be extrapolated to colder temperatures by incurring a small addition in uncertainty. Results from this work would facilitate the detection of *trans*-2-C_4H_8 in Titan's stratosphere, through ground-based and space-based observations (e.g. IRTF/TEXES, Cassini CIRS, JWST/MIRI). Confirming the presence or absence of *trans*-2-butene in Titan's atmosphere can inform future work aimed at understanding haze formation, the formation and composition of Titan's lakes and seas, and constraining reactions involving the chiral molecule *trans*-1,2-dimethylcyclopropane, perhaps through future measurements from Dragonfly's DraMS instrument [53].

Declaration of competing interest

The authors declare that they have no known competing financial interests or personal relationships that could have appeared to influence the work reported in this paper.

Data availability

Data will be made available on request

Acknowledgments

This research was sponsored by the National Aeronautics and Space Administration, United States (NASA) through a contract with ORAU. The material is based upon work supported by NASA, United States under award number 80GSFC21M0002. The views and conclusions contained in this document are those of the authors and should not be interpreted as representing the official policies, either expressed or implied, of the National Aeronautics and Space Administration (NASA) or the U.S. Government. The U.S. Government is authorized to reproduce and distribute reprints for Government purposes notwithstanding any copyright notation herein. Part of the research described in this article was performed at the Jet Propulsion Laboratory, California Institute of Technology under contracts with the National Aeronautics and Space Administration (NASA). Brendan Steffens and K. Sung have been supported by the NASA Cassini Data Analysis Program (CDAP). Brendan Steffens also wishes to thank the JPL Education Office and internship program for their administrative support. Rosaly Lopes, Michael Malaska, and Conor Nixon were supported by the NASA Astrobiology Institute, United States through the JPL-led team entitled Habitability of Hydrocarbon Worlds: Titan and Beyond. Conor Nixon was also supported by NASA's Solar System Observations Program.

References

[1] Trainer MG, Pavlov AA, Curtis DB, Mckay CP, Worsnop DR, Delia AE, et al. Haze aerosols in the atmosphere of early Earth: Manna from heaven. Astrobiology 2004;4(4):409–19. http://dx.doi.org/10.1089/ast.2004.4.409.

[2] Raulin F. Question 2: Why an Astrobiological study of Titan will help us understand the origin of life. Origins Life Evol Biospheres 2007;37(4–5):345–9. http://dx.doi.org/10.1007/s11084-007-9077-2, URL http://link.springer.com/10.1007/s11084-007-9077-2.

[3] Raulin F. Astrobiology and habitability of Titan. Space Sci Rev 2008;135(1–4):37–48. http://dx.doi.org/10.1007/s11214-006-9133-7, URL http://link.springer.com/10.1007/s11214-006-9133-7.

[4] Willacy K, Allen M, Yung Y. A new astrobiological model of the atmosphere of Titan. Astrophys J 2016;829(2):79. http://dx.doi.org/10.3847/0004-637X/829/2/79.

[5] Clarke DW, Ferris JP. Chemical evolution on Titan: Comparisons to the prebiotic earth. In: Whittet DCB, editor. Planetary and interstellar processes relevant to the origins of life. Dordrecht: Springer Netherlands; 1997, p. 225–48.

[6] Trainer M. Atmospheric prebiotic chemistry and organic Hazes. Curr Org Chem 2013;17(16):1710–23. http://dx.doi.org/10.2174/13852728113179990078.

[7] Hanel R. Infrared observations of the saturnian system from Voyager 1. Science 1981.

[8] Brown R. Titan from Cassini-Huygens. Springer; 2009.

[9] Coustenis A, Taylor F. Titan - Exploring an Earthlike world. World Scientific; 2008.

[10] Hörst SM. Titan's atmosphere and climate: Titan's atmosphere. J Geophys Res: Planets 2017;122(3):432–82. http://dx.doi.org/10.1002/2016JE005240, URL http://doi.wiley.com/10.1002/2016JE005240.

[11] Niemann HB, Atreya SK, Demick JE, Gautier D, Haberman JA, Harpold DN, et al. Composition of Titan's lower atmosphere and simple surface volatiles as measured by the Cassini-Huygens probe gas chromatograph mass spectrometer experiment. J Geophys Res 2010;115(E12):E12006. http://dx.doi.org/10.1029/2010JE003659, URL http://doi.wiley.com/10.1029/2010JE003659.

[12] Flasar FM, Kunde VG, Abbas MM, Achterberg RK, Ade P, Barucci A, et al. Exploring the Saturn system in the thermal infrared: The composite infrared spectrometer. Space Sci Rev 2004;129.

[13] Jennings DE, Flasar FM, Kunde VG, Nixon CA, Segura ME, Gorius NJP, et al. The composite infrared spectrometer (CIRS) on Cassini. Appl Opt 2017;56(18):5274–94.

[14] Kessler M. The infrared space observatory (ISO) mission. Adv Space Res 2002;30(9):1957–65. http://dx.doi.org/10.1016/S0273-1177(02)00557-4, URL https://linkinghub.elsevier.com/retrieve/pii/S0273117702005574.

[15] Lacy J, Richter M, Greathouse T, Jaffe D, Zhu Q. TEXES: A sensitive high-resolution grating spectrograph for the mid-infrared. Publ Astron Soc Pac 2002;114(792):153–68. http://dx.doi.org/10.1086/338730, URL http://iopscience.iop.org/article/10.1086/338730.

[16] Nixon CA, Thelen AE, Cordiner MA, Kisiel Z, Charnley SB, Molter EM, et al. Detection of cyclopropenylidene on Titan with ALMA. Astron J 2020;160(5):205. http://dx.doi.org/10.3847/1538-3881/abb679, URL https://iopscience.iop.org/article/10.3847/1538-3881/abb679.

[17] Sung K, Toon GC, Mantz AW, Smith MAH. FT-IR measurements of cold C3H8 cross sections at 7–15 μm for Titan atmosphere. Icarus 2013;226(2):1499–513. http://dx.doi.org/10.1016/j.icarus.2013.07.028, URL https://linkinghub.elsevier.com/retrieve/pii/S0019103513003291.

[18] Sung K, Toon GC, Drouin BJ, Mantz AW, Smith MAH. FT-IR measurements of cold propene (C3H6) cross-sections at temperatures between 150 and 299 K. J Quant Spectrosc Radiat Transfer 2018;213:119–32. http://dx.doi.org/10.1016/j.jqsrt.2018.03.011, URL https://linkinghub.elsevier.com/retrieve/pii/S0022407317307306.

[19] Sung K, Steffens B, Toon G, Nemchick D, Smith MA. Pseudoline parameters to represent n-butane (n-C4H10) cross-sections measured in the 7-15 μm region for the Titan atmosphere. J Quant Spectrosc Radiat Transfer 2020;107011. http://dx.doi.org/10.1016/j.jqsrt.2020.107011, URL https://linkinghub.elsevier.com/retrieve/pii/S0022407320301539.

[20] Yung YL, Allen M, Pinto JP. Photochemistry of the atmosphere of Titan - Comparison between model and observations. Astrophys J Suppl Ser 1984;55:465. http://dx.doi.org/10.1086/190963, URL http://adsabs.harvard.edu/doi/10.1086/190963.

[21] Vuitton V, Yelle R, Klippenstein S, Hörst S, Lavvas P. Simulating the density of organic species in the atmosphere of Titan with a coupled ion-neutral photochemical model. Icarus 2019;324:120–97. http://dx.doi.org/10.1016/j.icarus.2018.06.013, URL https://linkinghub.elsevier.com/retrieve/pii/S0019103517307522.

[22] Dobrijevic M, Loison J, Hue V, Cavalié T. One dimension photochemical models in global mean conditions in question: Application to Titan. Icarus 2021;364:114477. http://dx.doi.org/10.1016/j.icarus.2021.114477, URL https://linkinghub.elsevier.com/retrieve/pii/S0019103521001573.

[23] Cordier D, Mousis O, Lunine JI, Lavvas P, Vuitton V. An estimate of the chemical composition of Titan's lakes. Astrophys J 2009;707(2):L128–31. http://dx.doi.org/10.1088/0004-637X/707/2/L128, URL https://iopscience.iop.org/article/10.1088/0004-637X/707/2/L128.

[24] Hayes AG. The lakes and seas of Titan. Ann Rev Earth Planet Sci 2016;44(1):57–83. http://dx.doi.org/10.1146/annurev-earth-060115-012247, URL http://www.annualreviews.org/doi/10.1146/annurev-earth-060115-012247.

[25] Kim YS, Bennett CJ, Chen L-H, O'Brien K, Kaiser RI. Laboratory studies on the irradiation of solid ethane analog ices and implications to Titan's chemistry. Astrophys J 2010;711(2):744–56. http://dx.doi.org/10.1088/0004-637X/711/2/744, URL https://iopscience.iop.org/article/10.1088/0004-637X/711/2/744.

[26] Loison JC. The photochemical production of aromatics in the atmosphere of Titan. Icarus 2019;17.

[27] Willacy K, Chen S, Adams DJ, Yung YL. Astrophys J 2021. Accepted- Private communication with Yuk Yung at California Institute of Technology.

[28] Krasnopolsky VA. A photochemical model of Titan's atmosphere and ionosphere. Icarus 2009;201(1):226–56. http://dx.doi.org/10.1016/j.icarus.2008.12.038, URL https://linkinghub.elsevier.com/retrieve/pii/S0019103509000062.

[29] Nixon CA, Achterberg RK, Ádámkovics M, Bézard B, Bjoraker GL, Cornet T, et al. Titan science with the James Webb space telescope. Publ Astron Soc Pac 2016;128(959):018007. http://dx.doi.org/10.1088/1538-3873/128/959/018007, URL https://iopscience.iop.org/article/10.1088/1538-3873/128/959/018007.

[30] Gordon IE, Rothman LS, Hargreaves RJ, Hashemi R, Karlovets EV, Skinner FM, et al. The HITRAN2020 molecular spectroscopic database. J Quant Spectrosc Radiat Transfer 2022;277:107949. http://dx.doi.org/10.1016/j.jqsrt.2021.107949.

[31] Shimanouchi T, Standards USNBo, Commerce USDo. Tables of molecular vibrational frequencies. In: NSRDS-NBS, (no. pt. 1). National Bureau of Standards; 1972, URL https://books.google.com/books?id=9NZEAAAAIAAJ.

[32] McKean D, Mackenzie M, Morrisson A, Lavelley J, Janin A, Fawcett V, et al. Vibrational spectra of cis and transe but-2-enes: Assignments, isolated CH stretching frequencies and CH bond lengths. Spectrochim Acta 1985;41A(3):435–50.

[33] Chhiba M, Vergoten G. The structures and vibrational frequencies of a series of linear alkenes obtained using the spectroscopic potential SPASIBA. J Mol Struct 1994;326:35–8.

[34] Derreumaux P, Vergoten G. A new spectroscopic molecular mechanics force field. Parameters for proteins. J Chem Phys 1995;102(21):8586–605. http://dx.doi.org/10.1063/1.468848.

[35] Bell S, Drew B, Guirgis G, Durig J. The far infrared spectrum, ab initio calculations and conformational energy differences of 1-butene. J. Mol Struct 2000;553(1–3):199–219. http://dx.doi.org/10.1016/S0022-2860(00)00572-X, URL https://linkinghub.elsevier.com/retrieve/pii/S002228600000572X.

[36] Barnes AJ, Howells JDR. Infra-red cryogenic studies. Part 12.—Alkenes in argon matrices. J Chem Soc, Faraday Trans 2 1973;69:532–9. http://dx.doi.org/10.1039/F29736900532, URL http://dx.doi.org/10.1039/F29736900532.

[37] Gillett FC, Forrest W, Merrill K. Further observations of the 8-13 micron spectrum of Titan. Astrophys J 1975;201:L41. http://dx.doi.org/10.1086/181937, URL http://adsabs.harvard.edu/doi/10.1086/181937.

[38] Sharpe SW, Johnson TJ, Sams RL, Chu PM, Rhoderick GC, Johnson PA. Gas-phase databases for quantitative infrared spectroscopy. Appl Spectrosc 2004;58(12):1452–61. http://dx.doi.org/10.1366/0003702042641281, URL http://journals.sagepub.com/doi/10.1366/0003702042641281.

[39] Varanasi P. Intensities of the fundamental bands of the nu sub 3 system in CO2 and N2O spectra. In: Heat Mass Transf - V. 8, 1977, p. 191–5.

[40] Varanasi P, Chudamani S. Self- and N_2-broadened spectra of water vapor between 7.5 and 14.5 μm. J Quant Spectrosc Radiat Transfer 1987;38:407–12. http://dx.doi.org/10.1016/0022-4073(87)90094-X.

[41] Toon GC, Farmer CB, Schaper PW, Lowes LL, Norton RH. Composition measurements of the 1989 Arctic winter stratosphere by airborne infrared solar absorption spectroscopy. J Geophys Res: Atmos 1992;97(D8):7939–61. http://dx.doi.org/10.1029/91JD03114, URL https://agupubs.onlinelibrary.wiley.com/doi/abs/10.1029/91JD03114.

[42] Toon GC, Blavier J-F, Sen B, Margitan JJ, Webster CR, May RD, et al. Comparison of MkIV balloon and ER-2 aircraft measurements of atmospheric trace gases. J Geophys Res: Atmos 1999;104(D21):26779–90. http://dx.doi.org/10.1029/1999JD900379, URL http://doi.wiley.com/10.1029/1999JD900379.

[43] Sung K, Toon GC, Crawford TJ. N2- and (H2+He)-broadened cross sections of benzene (C6H6) in the 7–15 μm region for the Titan and Jovian atmospheres. Icarus 2016;271:438–52. http://dx.doi.org/10.1016/j.icarus.2016.01.012, URL https://linkinghub.elsevier.com/retrieve/pii/S0019103516000166.

[44] Nixon C, Jennings D, Flaud J-M, Bézard B, Teanby N, Irwin P, et al. Titan's prolific propane: The Cassini CIRS perspective. Planet Space Sci 2009;57(13):1573–85. http://dx.doi.org/10.1016/j.pss.2009.06.021, URL https://linkinghub.elsevier.com/retrieve/pii/S0032063309001925.

[45] Nixon CA, Jennings DE, Bézard B, Vinatier S, Teanby NA, Sung K, et al. Detection of propene in Titan's stratosphere. Astrophys J 2013;776(1):L14. http://dx.doi.org/10.1088/2041-8205/776/1/L14, URL https://iopscience.iop.org/article/10.1088/2041-8205/776/1/L14.

[46] Steffens BL, Nixon CA, Sung K, Irwin PGJ, Lombardo NA, Pereira E. New constraints on Titan's stratospheric n-butane abundance. Planet Sci J 2022;3(3):59. http://dx.doi.org/10.3847/PSJ/ac53ad, URL https://iopscience.iop.org/article/10.3847/PSJ/ac53ad.

[47] Nadler S, Jennings D. Foreign-gas pressure broadening parameters of propane near 748 cm-1. J Quant Spectrosc Radiat Transfer 1989;42(5):399–403. http://dx.doi.org/10.1016/0022-4073(89)90007-1, URL https://www.sciencedirect.com/science/article/pii/0022407389900071.

[48] Ding Y, Su W-W, Johnson SE, Strand CL, Hanson RK. Temperature-dependent absorption cross section measurements for propene, 1-butene, cis-/trans-2-butene, isobutene and 1,3-butadiene in the spectral region 8.4–11.7 μm. J Quant Spectrosc Radiat Transfer 2020;255:107240. http://dx.doi.org/10.1016/j.jqsrt.2020.107240, URL https://linkinghub.elsevier.com/retrieve/pii/S0022407320303411.

[49] Hayes A, Aharonson O, Callahan P, Elachi C, Gim Y, Kirk R, et al. Hydrocarbon lakes on Titan: Distribution and interaction with a porous regolith. Geophys Res Lett 2008;35(9):L09204. http://dx.doi.org/10.1029/2008GL033409, URL http://doi.wiley.com/10.1029/2008GL033409.

[50] Lopes RM, Peckyno RS, Le Gall AA, Wye L, Stofan ER, Radebaugh J, et al. Titan's methane cycle and its effect on surface geology. In: AGU fall meeting abstracts, vol. 2010, 2010, p. P31C–1548.

[51] Woodworth RC, Skell PS. Methylene, CH2. Stereospecific reaction with cis- and trans-2-butene. J Am Chem Soc 1959;81(13):3383–6. http://dx.doi.org/10.1021/ja01522a058.

[52] Bader RFW, Generosa JI. The chemistry of singlet and triplet methylene. Can J Chem 1965;43(6):1631–44. http://dx.doi.org/10.1139/v65-215, URL http://www.nrcresearchpress.com/doi/10.1139/v65-215.

[53] Trainer M, Brinckerhoff WB, Grubisic A, Danell R, Kaplan D. Development of the dragonfly mass spectrometer (DraMS) for Titan. In: LPI Contrib. No. 2548. 2021, p. 1532.